Poster presented at the
EuroWinter School "Observing with the VLTI"
February 3-8, 2002, Les Houches

Radiation Hydrodynamics Simulations of the Convective Envelope of Betelgeuse

Bernd Freytag

Department for Astronomy and Space Physics
at Uppsala University, Sweden,
[Bernd.Freytag@astro.uu.se]

Abstract

The spatial inhomogeneities on the surface of Betelgeuse revealed by interferometric observations are typically modelled as zero to three hot spots on a circular disk. While the surface structure appears to be generally consistent with an explanation as large-scale granular intensity fluctuations, the nature of the spots remains unclear.

The newly developed code COBOLD is now able to perform 3D radiation hydrodynamics simulations of a red supergiant, including realistic but simplified microphysics and non-local radiation transport.

The resulting models show giant convection cells, each covering a significant fraction of the stellar surface. However, these cells have more complex sub structures and a higher contrast than solar granules.

Some prominent features might be interpreted as hot spots in low-resolution observations. To reveal the true nature of the spots observations with higher spatial and some temporal resolution are necessary – supplemented by detailed numerical models.

Introduction: Some Facts about Betelgeuse

Parameters

- α Orionis, HD39801, HIP27989
- M2 Iab Supergiant
- Star with largest apparent diameter (after the Sun)
- Distance $d_{\rm Hipparcos}$=131±30 pc
- Apparent radius R=22.1 mas ⇒ R=620 $R_\odot$
- M=6 $M_\odot$, $T_{\rm eff}$=3600 K, $\log g$=-0.5,
  (or M=15 $M_\odot$, $T_{\rm eff}$=3500 K, $\log g$=0.0)
- Solar atmospheric composition

Observations

Observations reveal temporal brightness fluctuations, an extended hot atmosphere, and an irregular temporally variable surface structure (for some examples see Fig. 1).

By now, there are photometric data available covering a time span of almost 100 years. They come from various short-term photometric campaigns and from collected observations of amateur astronomers (Leo Goldberg 1984, PASP 96, 366). The overall brightness of Betelgeuse varies on time-scales of weeks, months, and years.

Observations with optical interferometers started 12 years ago. They still have an extremely low resolution but definitely show deviations of the image from circular symmetry. The measurements can be fitted by a model comprising a circular disc plus 0 to 3 bright spot(s). Fig. 1 shows a set of images l generated from the spot parameters from Buscher et al., 1990, MNRAS 245, 7p; Wilson et al., 1992, MNRAS 257, 369; Tuthill et al., 1997, MNRAS 285, 529; Wilson et al., 1997, MNRAS 291, 819 (their paper title became the headline of my Fig. 1); Klueckers et al., 1997, MNRAS 284, 711; Burns et al., 1997, MNRAS 290, L11; Young et al., 2000, MNRAS 315, 635.

In the last paper, the possibility of a fit with a circular disk and a single *dark* spot is discussed.

Ronald L. Gilliland and Andrea K. Dupree took a direct UV image with HST (1996, ApJ 463, L29). The deviations from circular symmetry are obvious. The VLA radio-observations by Jeremy Lim, Chris L. Carilli, Stephen M. White, Anthony J. Beasley, Ralph G. Marson (1998, Nature 392, 575) cannot resolve the very surface of the star, but reveal an asymmetric extended outer atmosphere.

Spectra (even some spatial resolution is possible) indicate large atmospheric and chromospheric velocities. But in general, spectroscopic observations of Betelgeuse are difficult to interpret due to the lack of a reliable (3D) model atmosphere (see David F. Gray, 2000, ApJ 532, 487 for an attempt).

Some Theory

Based on simple scaling arguments, Martin Schwarzschild suggested in 1975 (ApJ 195, 137) that a few giant granules on the surface of Betelgeuse are the cause for the observed temporal brightness variations: if the typical horizontal extent of a granule is a fixed multiple of some characteristic vertical scale length (e.g. the pressure scale height), granules on a supergiant will be much larger than on the Sun, not only in absolute but also in relative size.

In the meantime pulsations, shocks, rotation, and magnetic fields have been invoked besides convection to be responsible for some of the observed phenomena.

The Changing Face of Betelgeuse

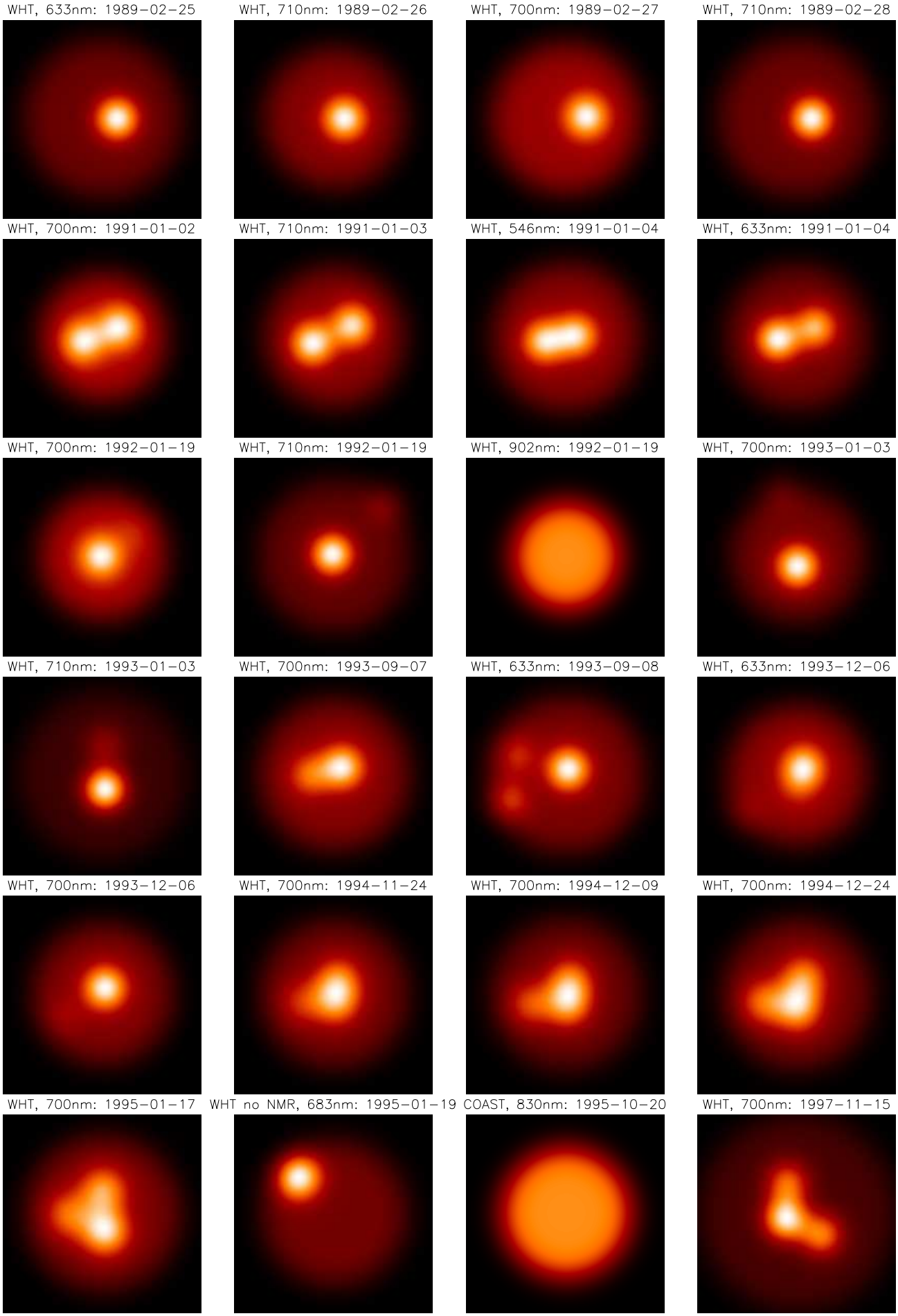

Figure 1: WHT and COAST observations in the visible and near IR. I compiled these images from the published data about spot positions and intensities.

Numerical Simulations with COBOLD

To produce a model of the outer layers of Betelgeuse, a new 3D radiation hydrodynamics code (CO^{5}BOLD: "COnservative COde for the COmputation of COmpressible COnvection in a BOx of L Dimensions, L=2,3") has been used, which can be described by some keywords:

Hydrodynamics Scheme

- Cartesian box: Operator (directional) splitting: 3D or 2D $\rightarrow$ 1D
- Approximate Riemann solver (Roe type)
- Including gravitation (external potential, non-split)
- Including ionization (tabulated EOS)
- Discrete conservation laws
- Reconstruction schemes of different order

Radiation Transport

- For single direction: equation of non-local radiative energy transfer solved with short-characteristics scheme
- 3 to 10 ray directions per sub-timestep
- Several sub-timesteps per global timestep possible
- Conservative energy transport
- Grey or frequency-dependent opacities (tabulated)
- No scattering, strict LTE

Setup for model st35gm04n04

To put the star in the box, a spherical potential for given stellar mass M_*=5 $M_\odot$, inner smoothing radius $r0_{\rm grav}$=135 $R_\odot$, and outer smoothing radius $r1_{\rm grav}$=1626 $R_\odot$ (well outside the computational domain) is prescribed by

$$\phi(r) = \frac{-G_{\rm grav} M_*}{\sqrt[4]{r0_{\rm grav}^4 + r^4 \sqrt{\frac{1}{1+\left(\frac{r^2}{r1_{\rm grav}^2}\right)^4}}}} \qquad (1)$$

with r as the distance to the center of the star. The computational volume is a cube with an edge length of 2×813$R_\odot$ and 171^3 grid points. This is so far the model with the highest resolution. Earlier ones were typically restricted to 127^3 points.

Within a sphere of radius $r0_{\rm grav}$ the internal energy is adjusted to keep the entropy close to a prescribed value (3.25 10^9 erg/K/g). This replaces the energy production by nuclear fusion in the real stellar core.

The outer boundaries are open, i.e. transmitting for waves.

The opacity tables rely on realistic data but are simple grey Rosseland means. They are a merger of the PHOENIX opacities (Hauschildt, P.H., Baron, E., Allard, F. 1997, ApJ 483, 390) and OPAL tables (Iglesias, C.A., Rogers, F.J., Wilson, B.G. 1992, ApJ 397, 717), kindly provided by Hans-Günter Ludwig.

The model is characterized by the parameters $T_{\rm eff}$∼3340 K, $\log g$∼-0.47, L_*∼46000 $L_\odot$.

The model turns out to be slightly to cool for Betelgeuse and is lies at the lower end of the allowed surface gravity range. Nevertheless, it already exhibits lots of features which likely play a role for the processes in the surface layers of the real star.

The simulations were performed on a SGI at TAC in Copenhagen, a Cray VX1 at the computer center at the CAU in Kiel, and on the new SunFire machines at the Ångström laboratory in Uppsala.

Results

Figure 2 shows a sequence of intensity snapshots from the very start of an earlier simulation (with 127^3 grid points and a long-characteristics radiation transport scheme). The initial model is a sphere in hydrostatic equilibrium. Due to convective instability a pattern of convective cells forms, which is initially symmetric but soon becomes irregular (see Fig. 3).

A sequence of entropy slices from the new model st35gm04n04 is presented in Fig. 5 which nicely shows the deep-reaching downdrafts. The temperature slices in Fig. 6 demonstrate the formation of shock waves in the atmosphere.

The comparison with a sequence from a fake star with solar surface parameters ($T_{\rm eff}$=5770 K, $\log g$=4.44) but the diameter of the Moon (Fig. 7) illustrates that the surface patterns differ significantly. Compared to solar granulation convection in a red supergiant is characterized by

- smaller ratio of radiative to hydrodynamical time-scales
- larger convective cells (measured in atmospheric pressure scale heights)
- increased convective velocities (with particularly strong tangential flows)
- pulsations interacting with convection, influencing the intensity pattern
- higher contrast of surface intensity, less obvious granular pattern

In the solar case (Fig. 7) small granules or the rims of some granules are the brightest structures. The surface images of the red supergiant (Fig. 4) are much more irregular. Some small bright features may have similar causes as in the solar granulation. However, the largest intensity contrast arises, when entire granules darken (e.g. at t=3.87 yrs, see also Fig.8). This happens, when the mass (and energy) flux through the surface of the granule is reduced – probably due to the influence of pulsations.

While cooler models show strong irregular global pulsations, the variations of the surface intensities of the newest model (cf. Fig. 9) are dominated by phenomena on shorter time scales – due to fluctuations of the granular pattern and/or small-wavelength pulsations.

Sequence I: Surface Intensity (Start)

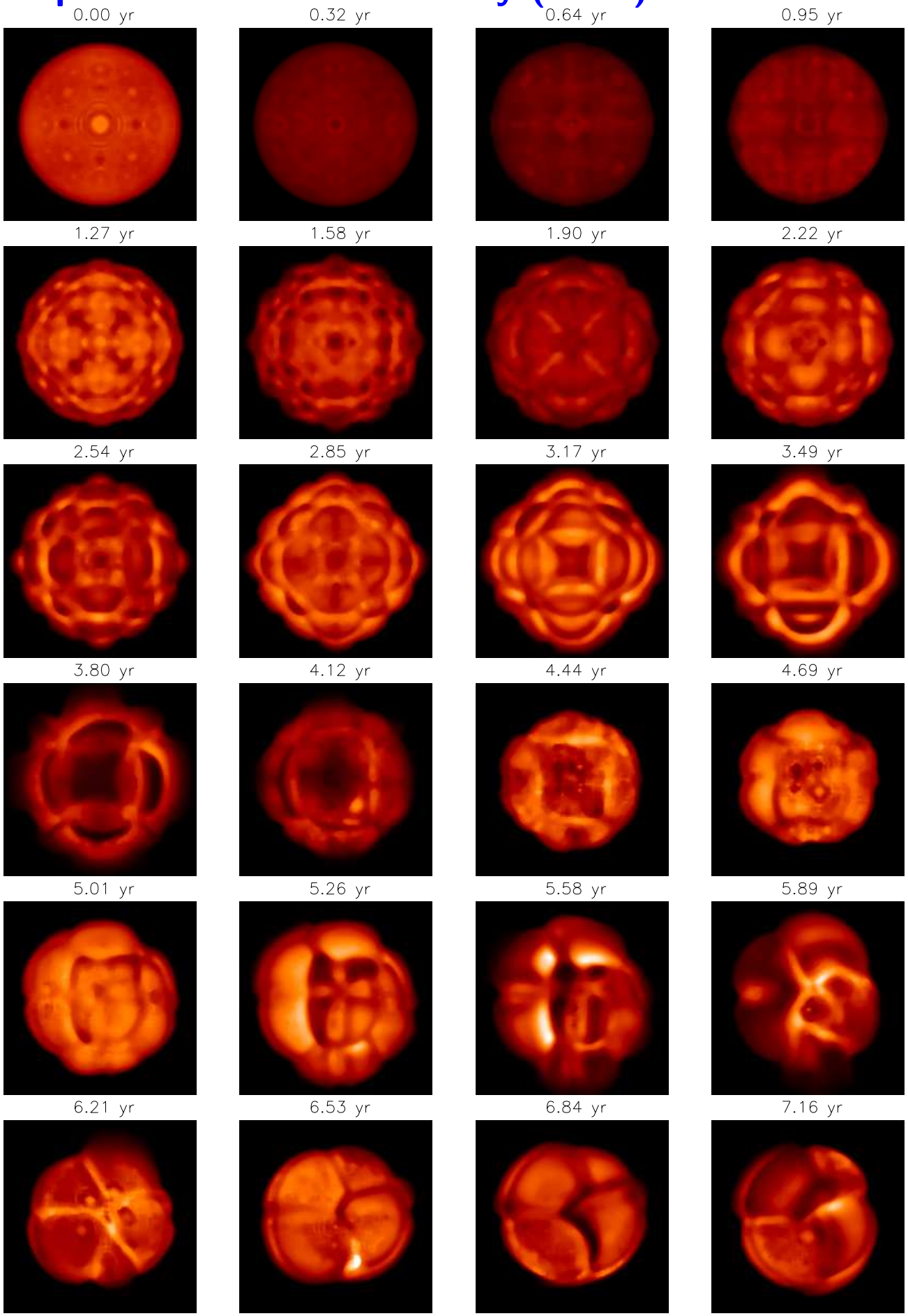

Figure 2: Sequence of surface intensity snapshots at start of simulation st33gm06n03. Parameters: $T_{\rm eff}$=3200 K, $\log g$=-0.5, 127^3 grid points. At the top the simulated stellar time is indicated in years.

Sequence II: Surface Intensity

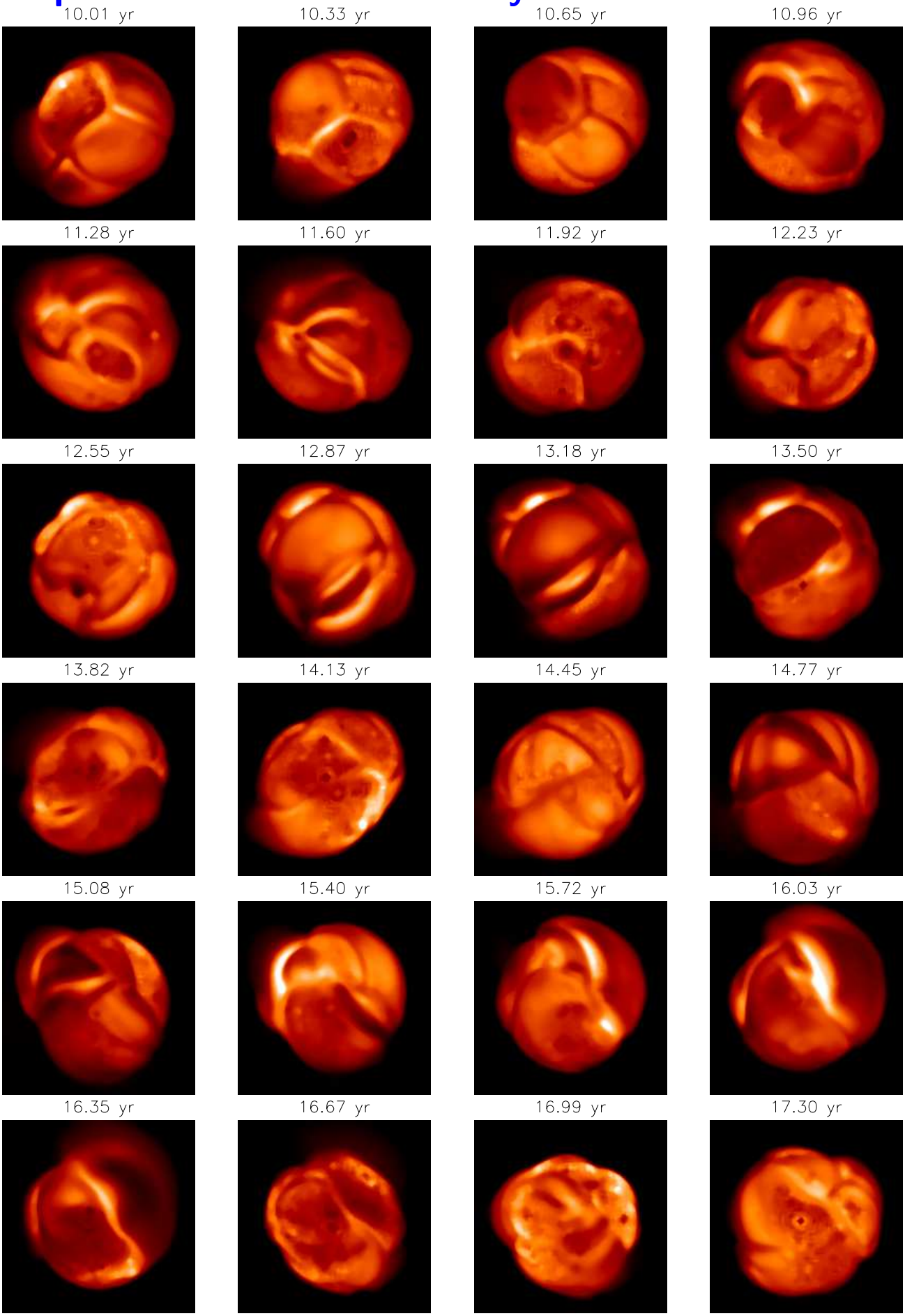

Figure 3: Surface intensity snapshots ($T_{\rm eff}$=3200 K, $\log g$=-0.5, 127^3 points). Sometimes, the cells are similar to solar granules (e.g. at 10.65 yrs.) But occasionally, there are bright features above downdrafts near disk center (16.03 yrs) or the at the rim (15.40 yrs).

Sequence III: Surface Intensity

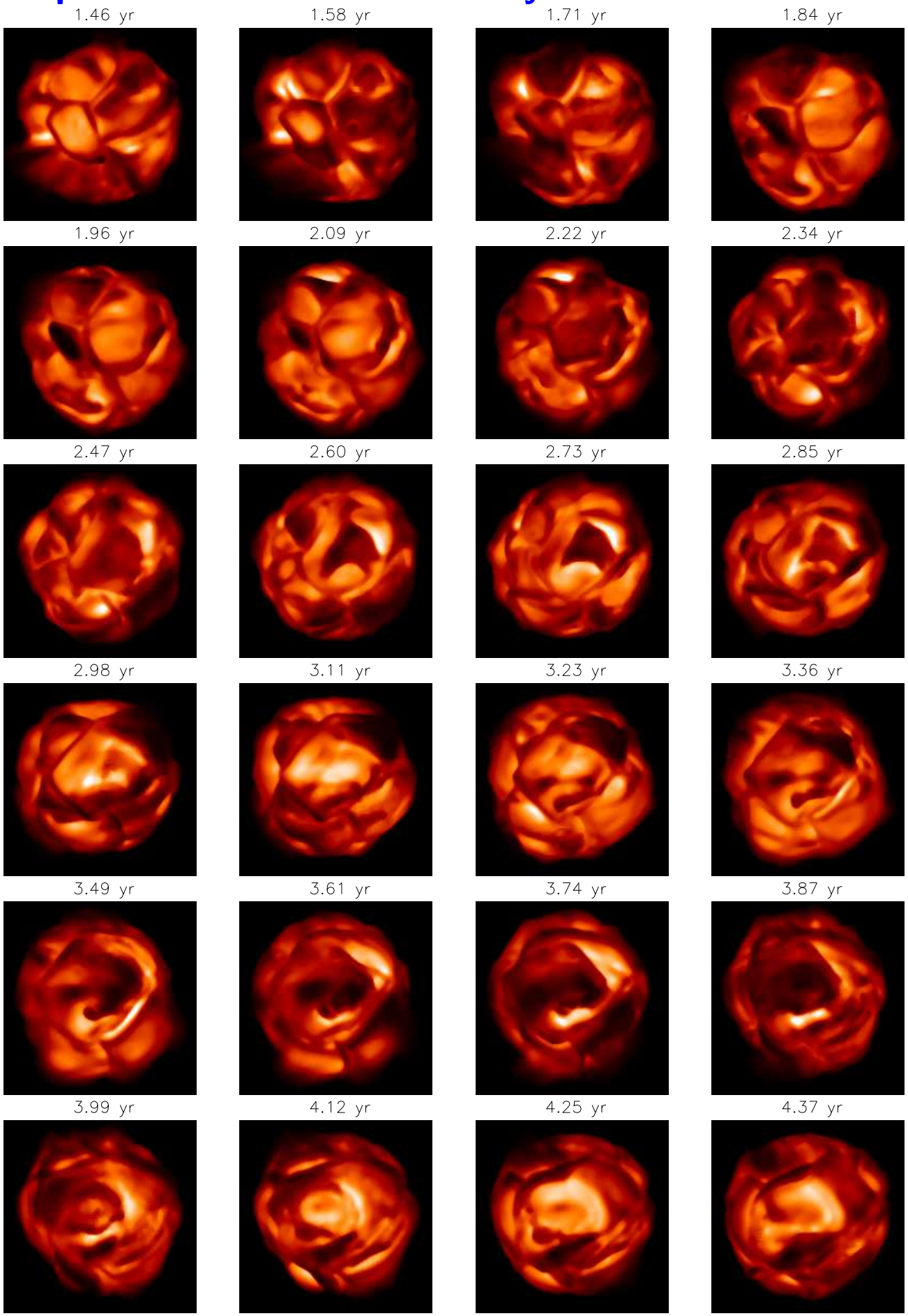

Figure 4: Sequence of surface intensity snapshots of the high-resolution model st35gm04n04 ($T_{\rm eff}$=3340 K, $\log g$=-0.47, 171^3 grid points).

Sequence III: Entropy Slices

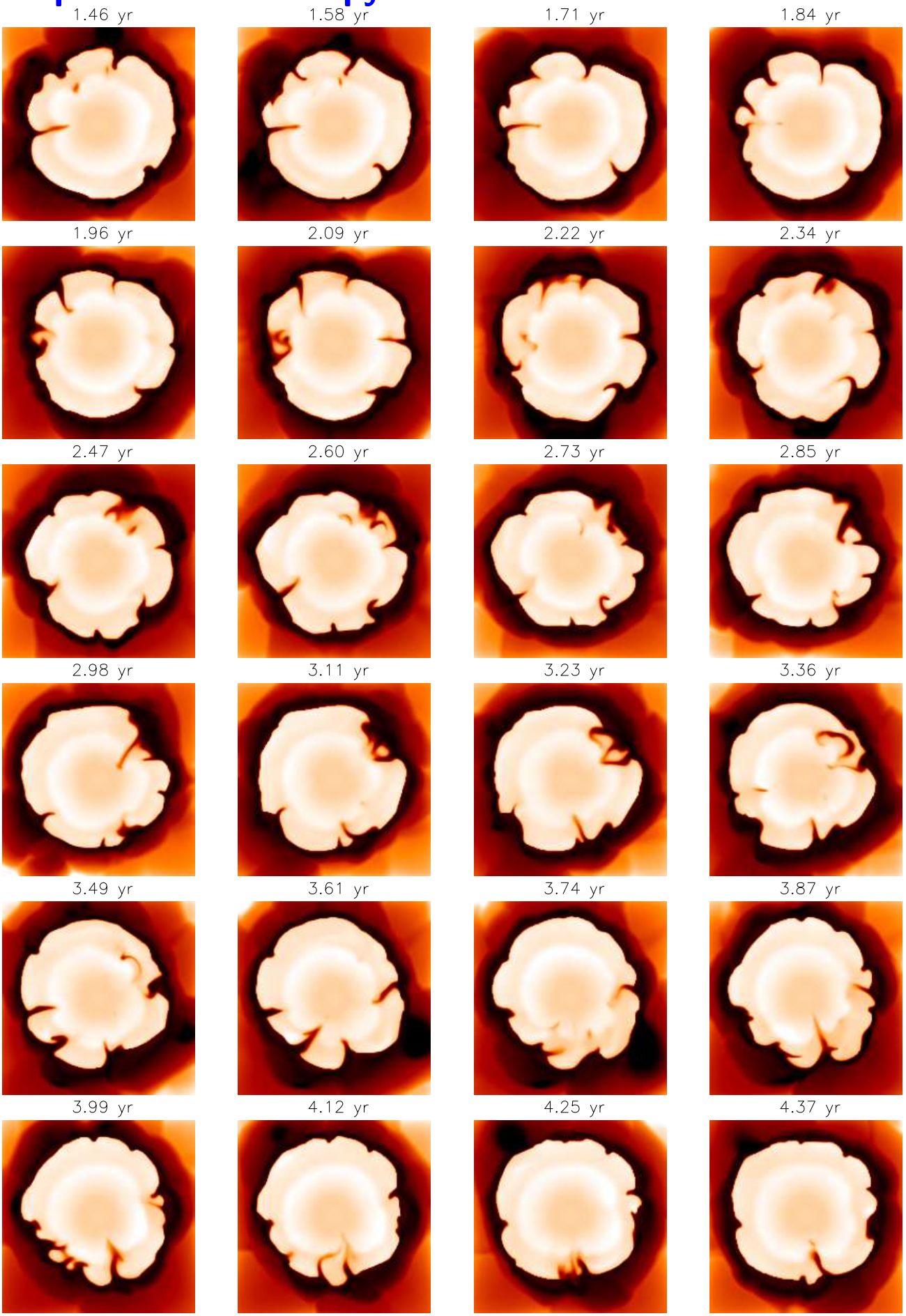

Figure 5: Sequence of entropy slices (st35gm04n04, $T_{\rm eff}$=3340 K, $\log g$=-0.47, 127^3 grid points). The star is not really spherically symmetric anymore. In a slice there are around 3 to 7 downdrafts, some of them reaching deep into the star.

Sequence III: Temperature Slices

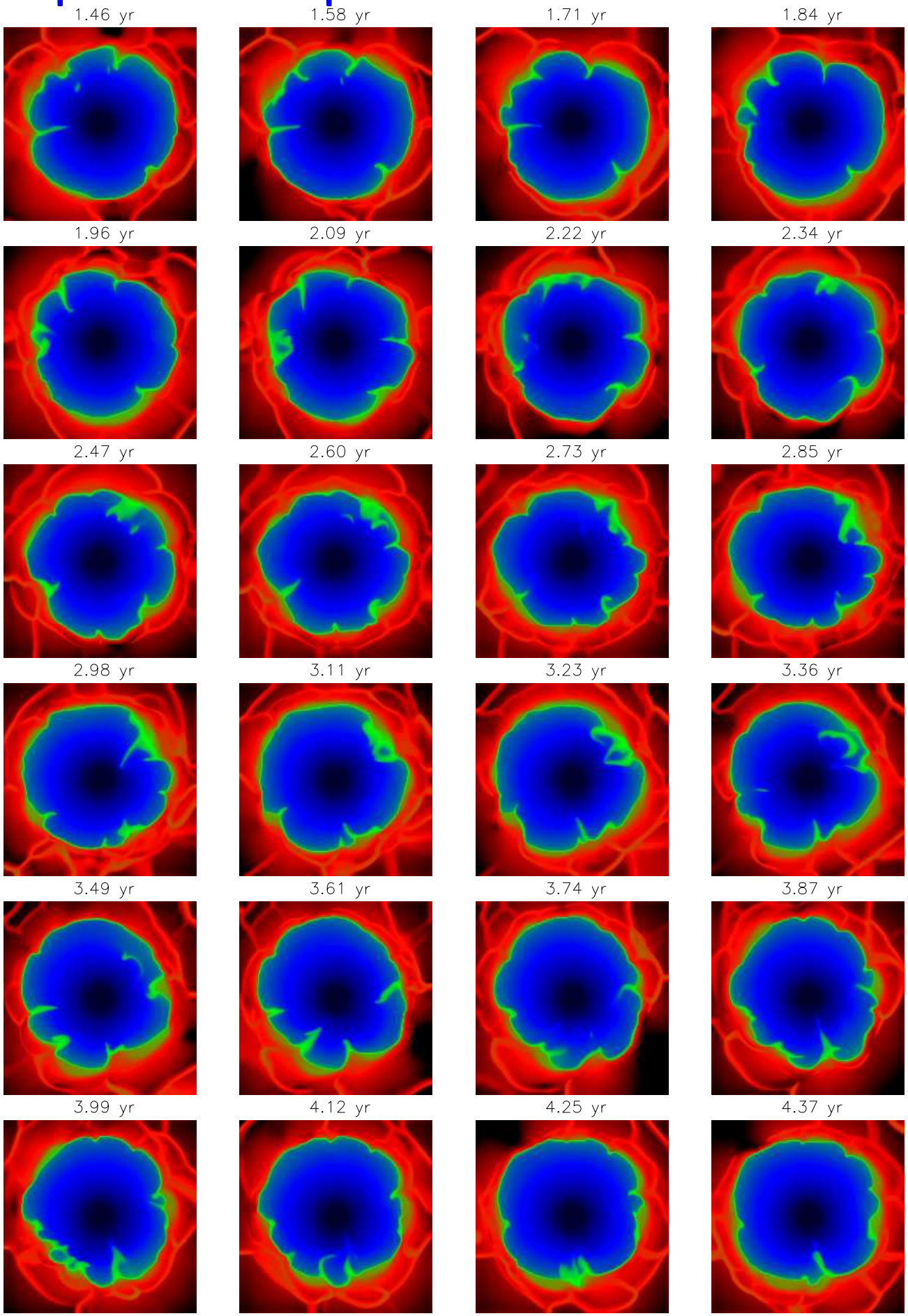

Figure 6: Sequence of temperature (ranging from 1500 K to 150 000 K) slices (st35gm04n04, $T_{\rm eff}$=3340 K, $\log g$=-0.47, 127^3 grid points). Shock waves run into the outer atmosphere, moving mainly radially.

Sequence IV: Surface Intensity (fake giant)

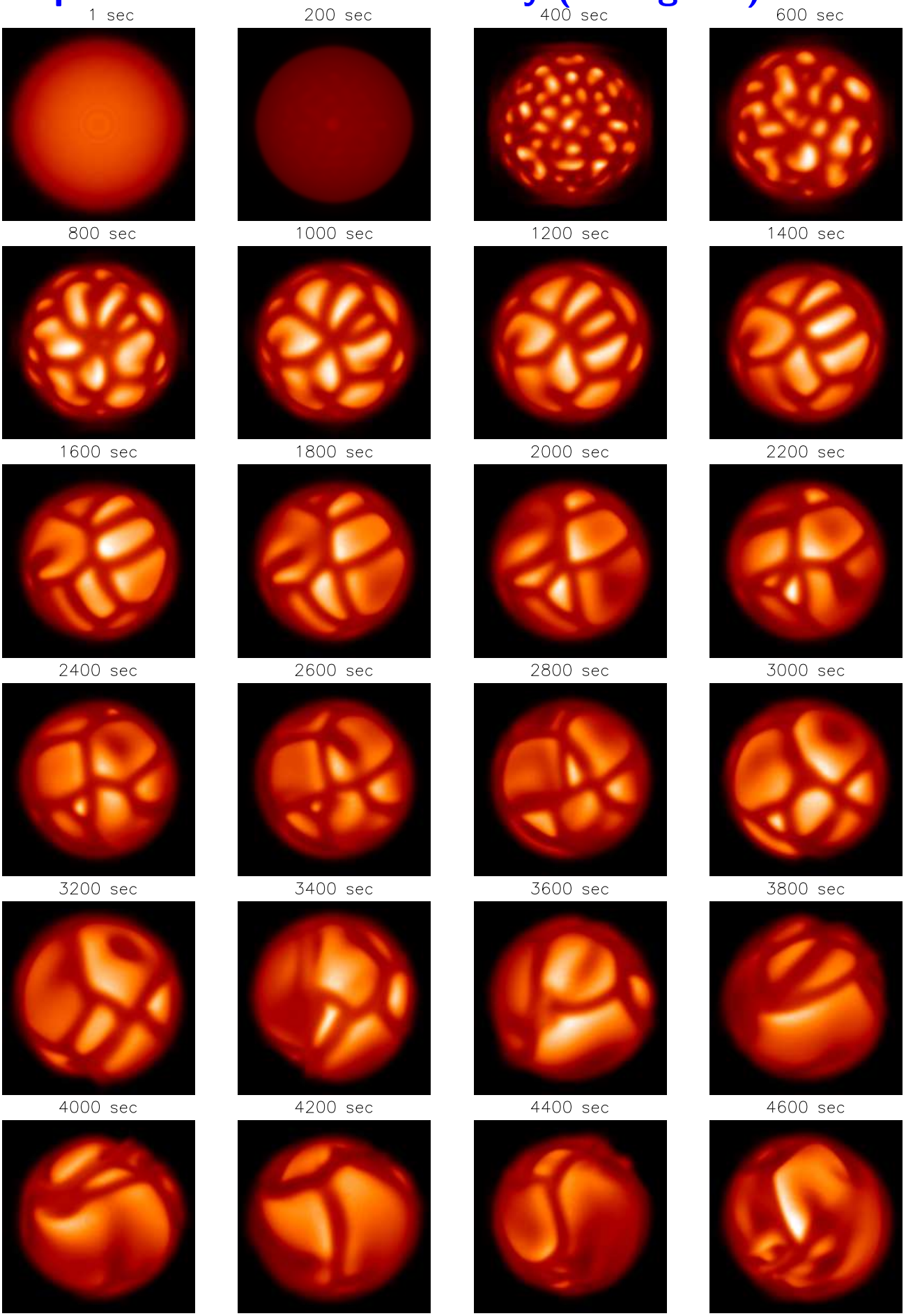

Figure 7: Sequence of surface intensity snapshots of comparison model st57g44n01-06. Surface parameters: $T_{\rm eff}$=5770 K, $\log g$=4.44, 127^3 grid points (the "solar" case). This is only a toy model with solar-size granulation wrapped around a moon-size object!

Filtered Intensity Images

To give an impression how an "observed surface image" of the simulated supergiant might look like a snapshot from Fig. 4 with dark granule and two small bright regions has been selected and smoothed with different filters. Even in the image with lowest resolution some features can be recognized. However, to allow the identification of the underlying physical processes a higher resolution is necessary.

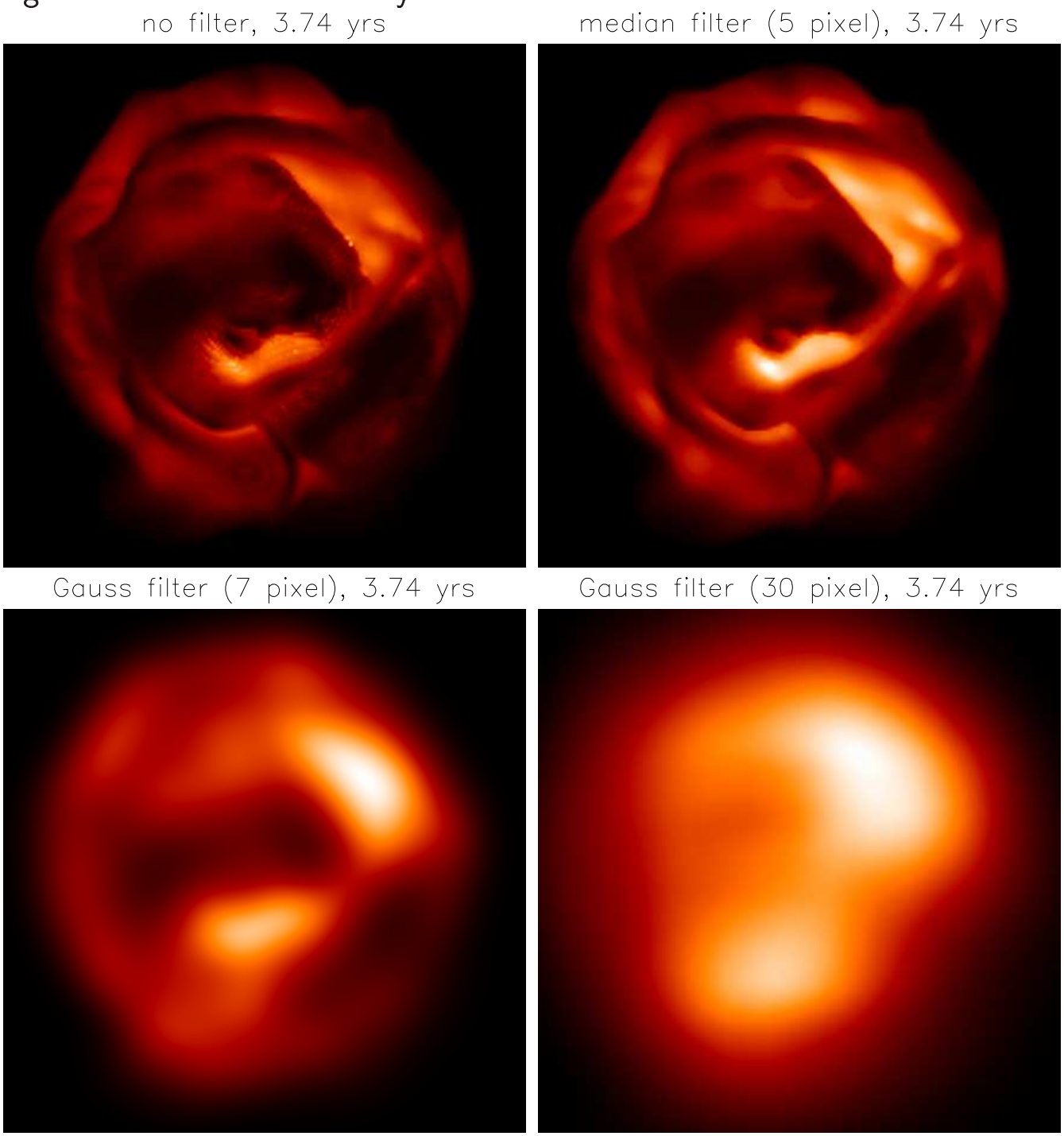

Figure 8: Selected surface intensity snapshot of high-resolution model (st35gm04n04, $T_{\rm eff}$=3340 K, $\log g$=-0.47, 171^3 grid points) with different degrees of smoothing: top left: no filtering, top right: median filter with small window to remove numerical artifacts, bottom left: Gaussian filter with σ=7 pixel ($k = \exp(-\frac{1}{2}(x^2+y^2)/\sigma^2)$), bottom right: strong Gaussian filter with σ=20 pixel. Each image has 171×171 pixel.

Time Variation of Intensity and Flux

The characteristic time-scale for fluctuations of the frequency-integrated intensity ($\approx$ 0.5 yrs) is shorter than the typical lifetime of a granule ($\geq$ 1 yr).

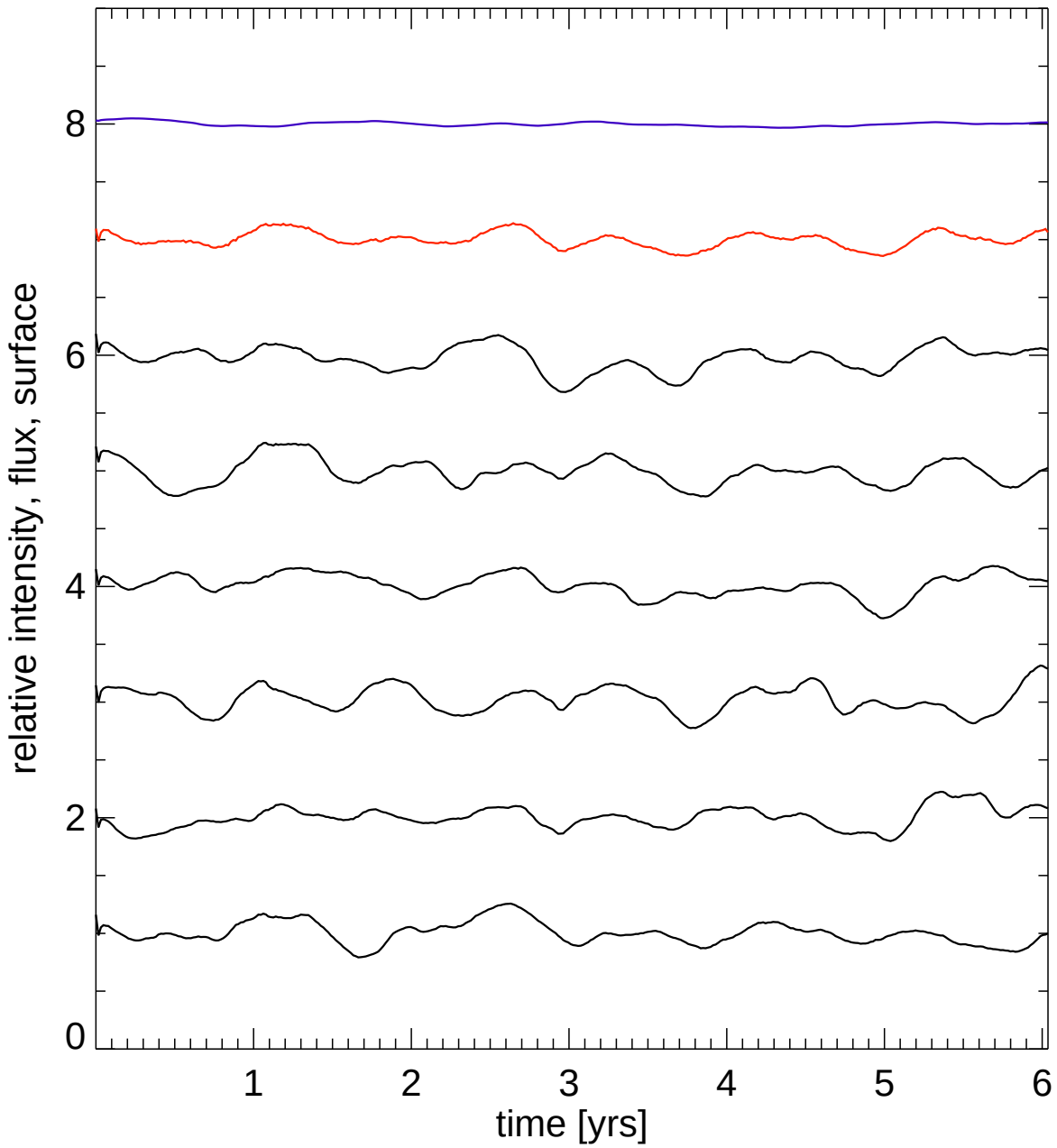

Figure 9: The relative surface intensities (shifted by 0,1,2,...,5) viewed from six different angles (lower black curves), the normalized and shifted total flux (red curve), and an estimate for the relative (and shifted) surface area (actually, the square of the mean radius, blue curve) are plotted for model st35gm04n04 with surface parameters $T_{\rm eff}$=3340 K, $\log g$=-0.47. Surface area variations play no significant role for the flux changes.

Conclusions

- 3D simulations of a red supergiant "star-in-a-box" including non-local radiative transfer with simplified realistic opacities are now feasible.
- A red supergiant (with low surface gravity $\log g \sim$-0.5) has only a few giant surface convection cells.
- The deviations from spherical symmetry of the star are significant.
- Atmospheric velocities are large. Shock waves are ubiquitous.
- Pulsations and their interaction with convection play an important role.
- The granulation appears not to be solar-like. The surface pattern is not simply composed of "bright granules and dark intergranular lanes". Instead, there are occasionally bright features (hot spots?) at the edges of granules or even over downdrafts. Entire granules can become significantly darker than the average leading to an intensity contrast exceeding the solar value.

Main Problems

- The short radiative time-scales make the computation of the radiation field very time-consuming.
- A high number of grid points is needed to resolve all features, particularly the steep temperature jump just below the photosphere.

Future Development

- A faster version of the code and access to more powerful computers are needed to allow a further increase of the number of grid points, frequency-bins,. . .
- Improved input physics (frequency-dependent opacities, radiation pressure, self-consistent gravity, dust, . . .) will lead to more realistic models.